Supporting information

Selective singlet oxygen generation by microporous biochar in peracetic acid activation

Selusiwe Ncube,[†a] Zhihao Tian,[†a] Shuhui Liu,[a] Shaobin Wang[a] and Wenjie Tian*[a]

[a] School of Chemical Engineering, The University of Adelaide, North Terrace, Adelaide, SA 5005, Australia

[†]Authors contribute equally.

[*]E-mail: wenjie.tian@adelaide.edu.au

Materials and Methods

Chemicals and reagents

Methanol (MeOH, ≥ 99%), ethanol absolute (EtOH, ≥ 99.5%), acetonitrile, phenol (≥ 99.5%), 4-chlorophenol (4-CP), 2,2,6,6-tetramethyl-4-piperidinol (TEMP, 98%), 5,5-dimethyl-1-pyrroline n-oxide (DMPO), *tert*-butyl alcohol (TBA, ≥ 99.5%), hydrochloric acid (HCl, 37%), sodium hydroxide (NaOH), isopropanol (99.7%), acetic acid, commercial steam activated charcoal Norit (AC), concentrated sulphuric acid (H_2SO_4) and H_2O_2 30% w/w, were purchased from Sigma-Aldrich. Nafion solution (5 wt.%) was sourced from Alfa Aesar. All the chemical reagents used for the experiments were of analytical grade. PAA was prepared by mixing H_2O_2 and CH_3COOH, with H_2SO_4 acting as a catalyst [1]. Unless otherwise indicated, ultra-pure water (18.2 mΩ cm^{-1}) was used to prepare the solutions throughout the experiments.

Material synthesis

The pappi of Common sow thistle (*Sonchus oleraceus L.*) were hand-picked around Adelaide, washed in deionized water and dried in an oven at 60 °C. The dried pappi was then transferred to an uncovered porcelain crucible and subjected to a one-pot pyrolysis process in a tube furnace for 3 h at 500, 600, 700, 800, 900 and 1000 °C and the resulting products cooled and ground to obtain N_2-C-500, N_2-C-600, N_2-C-700, N_2-C-800, N_2-C-900 and N_2-C-1000, respectively. Additionally, NH_3-C-900 and H_2-C-900 catalysts were synthesized using a similar method but under NH_3/Ar and H_2/Ar atmospheres, respectively, at 900 °C with a flow rate of 5°C/min. Commercial AC was ground to powder and used for comparison purposes.

Characterization of catalysts

Scanning electron microscopy (SEM, FEI Quanta 450 FEG) was used to investigate the morphologies of the obtained biochar samples. X-ray diffraction (XRD) was conducted using a Rigaku Mini Flex 600 X-ray diffractometer. Brunauer-Emmett-Teller (BET) analysis was used to analyze the surface area and porosity of the catalysts and surface characterization was conducted by evaluating the adsorption-desorption isotherms of liquid nitrogen at 77 K on ASAP 2460. The surface functional groups and the chemical composition were examined through X-ray photoelectron spectroscopy (XPS) (Thermo Scientific K-alpha). X-ray absorption near-edge structure (XANES) measurements were conducted at the Australian synchrotron, utilizing the soft X-ray spectroscopy beamline and spectra were normalized using Athena.

Experimental procedure

Adsorption and degradation experiments were conducted separately. Unless otherwise indicated, the concentrations of phenol, PAA and biochar were 5 ppm, 2 mM and 0.1 gL^{-1}, respectively, and the experiments were carried out at an initial pH of 7. The error bars denote the standard deviations from duplicate tests.

In adsorption tests, 0.1 g L^{-1} sample was added into the solution containing 5 ppm phenol with magnetic stirring at 250 rpm at room temperature.

Degradation experiments were performed in a 250 mL beaker containing a 75 ml solution of 5 ppm phenol with magnetic stirring. Typically, 2 mM PAA was added to the phenol solution and the pH adjusted to neutral using HCl and/or NaOH. The sample (0.1 gL^{-1}) was then added successively. Samples (1.0 mL) were taken at intervals from the reaction mixture, filtered and quenched with 0.5 mL of MeOH previously added in high-performance liquid chromatography (HPLC) vials. The reaction kinetics (k_{obs}) of phenol degradation was assumed to follow a first-order kinetic model (Eq. 1)

$$ln\frac{C_t}{C_0} = -k_{obs} \times t \tag{1}$$

where C_0 is the initial phenol concentration and C_t is the phenol concentration at time t.

Quenching experiments were performed to identify the reactive oxygen species (ROS) in the degradation process of phenol. Various quenching agents were introduced to the reaction, including EtOH (3 M), MeOH (0.5 M), TBA (100 mM) and L-histidine (L-his, 6 mM). For the stability tests, NH_3-C-900 was collected after each reaction, washed several times with EtOH and deionized water and dried at 60 °C.

Analytical methods

HPLC, Thermo Scientific was used to analyze the concentration of the micropollutants. The mobile phase consisted of acetonitrile and ultrapure water (30:70, v/v) with a flow rate of 1 mL min^{-1}. The ROS in the reaction and the degradation mechanism were evaluated through quenching experiments, electrochemical studies and electron paramagnetic resonance (EPR). EPR spectra were obtained using an ESR5000 spectrometer/ Bruker EMX plus-6/1, with TEMP and DMPO as trapping agents. The catalyst was dispersed in phenol solution and combined with PAA and the trapping agents, then drawn into an EPR glass capillary tube, which was then sealed on one end and inserted into the EPR sample chamber for testing.

Electrochemical measurements

Electrochemical measurements, including cyclic voltammetry (CV), linear sweep voltammetry (LSV) and current-time (I-t) measurements, and open circuit potential (OCP) tests were conducted on an electrochemical workstation (CHI760E). The catalyst ink was prepared by dispersing 4 mg of biochar in Nafion, 500 μL of water and 480 μL of 2-propanol under ultrasonication for 1 h. 20 μL of the ink was pipetted, loaded onto a glassy carbon electrode (GCE) and dried. The experiment was carried out in a 100 mL beaker containing 0.5 M Na_2SO_4 electrolyte solution to which 5 ppm phenol and 2 mM PAA at pH 7 were added in succession. The OCPs were monitored using a two-electrode system consisting of the prepared GCE as the working electrode and saturated Ag/AgCl electrode as the reference electrode. I-t curves, LSV and CV measurements were carried out using a three-electrode setup. A Pt electrode was used as the counter electrode. The saturated Ag/AgCl electrode was used as the reference electrode and GCE was used as the working electrode. LSV was conducted in a potential range of 0.2 - +2 V at a scan rate of 0.05 V s^{-1} and CV was carried out at a constant scanning rate of 0.05 Vs^{-1} between 1 and −1 V.

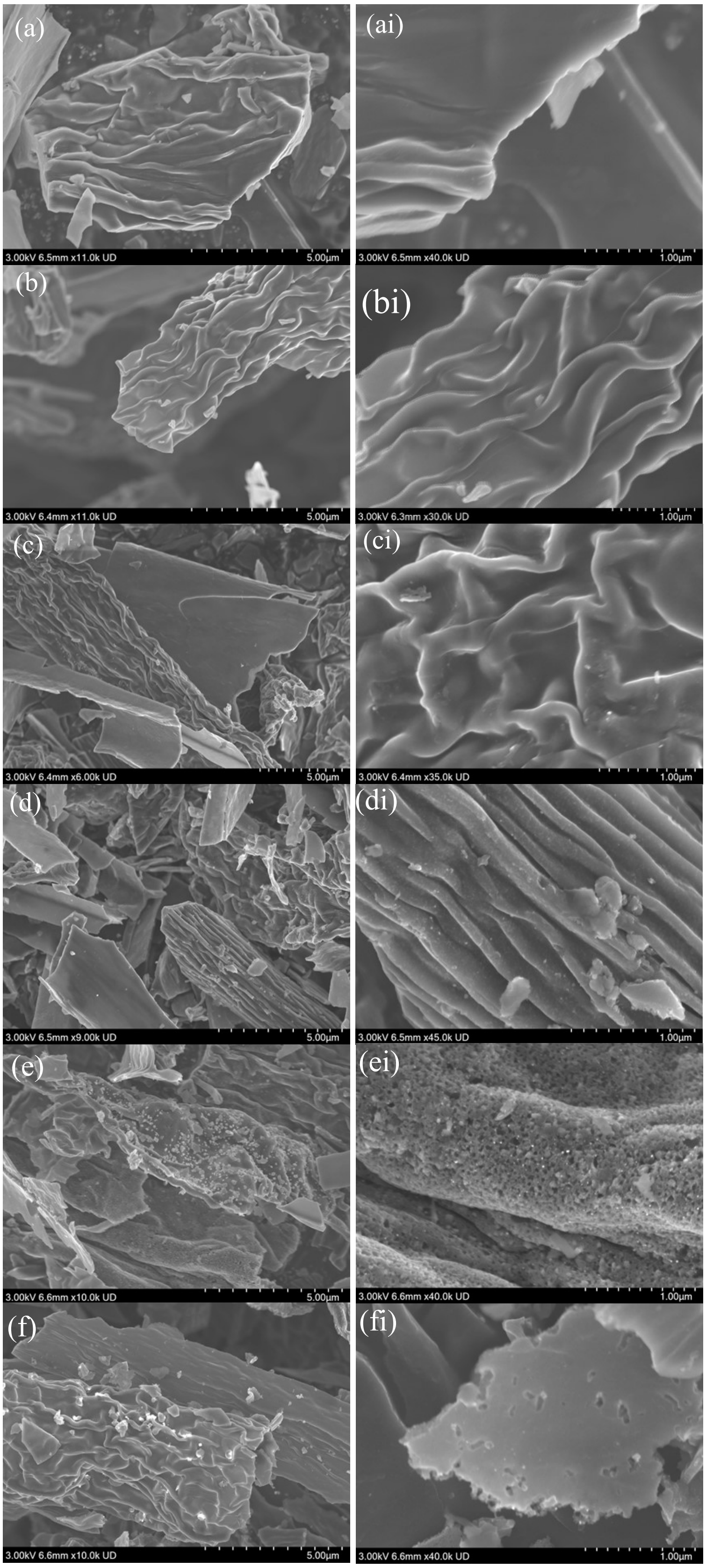

Fig. S1 SEM images of (a-ai) N_2-C-500, (b-bi) N_2-C-600, (c-ci) N_2-C-700, (d-di) N_2-C-800, (e-ei) N_2-C-900 and (f-fi) N_2-C-1000.

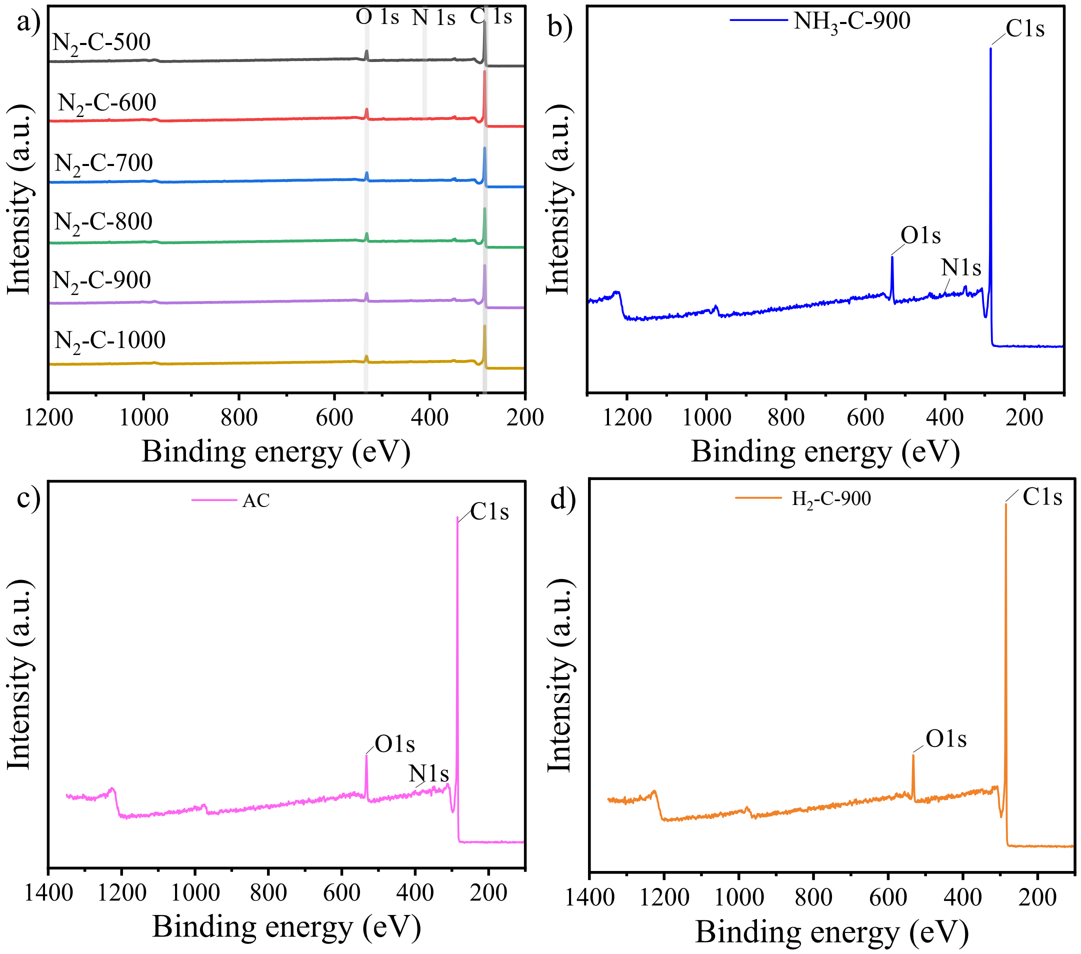

Fig. S2 XPS full survey spectra of a) N_2-C-x at different temperatures, b) NH_3-C-900, c) AC and d) H_2-C-900.

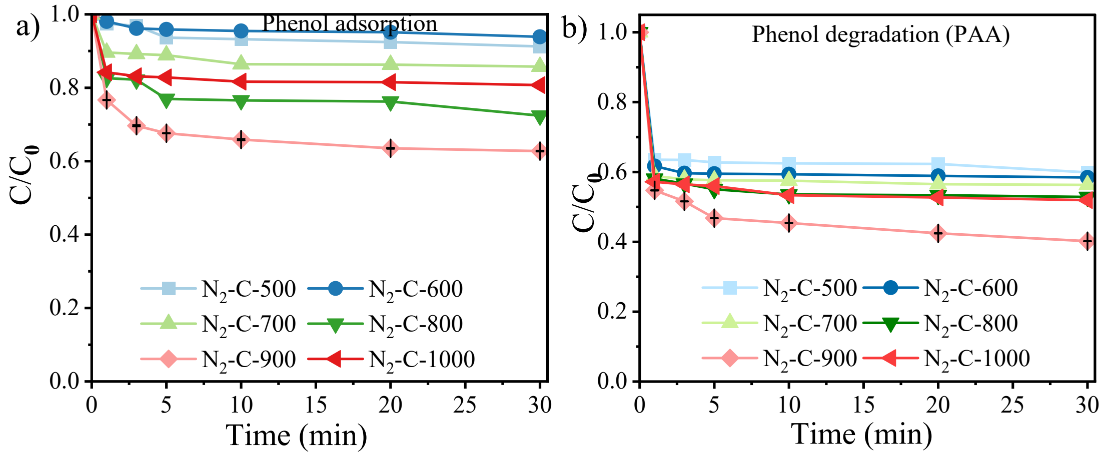

Fig. S3 a) Adsorption and b) degradation curves of catalysts synthesized under different temperatures (Experimental conditions: $[PAA]_0 = 2.0$ mM (where required), $[Catalyst\ ]_0 = 0.1$ gL^{-1}, [Phenol] = 5 ppm, T = 25 °C and $pH_0 = 7$)

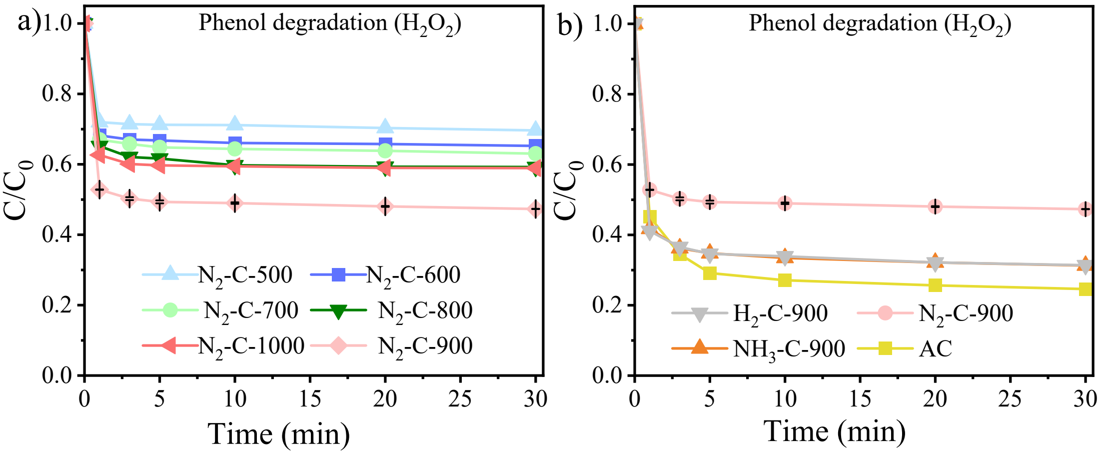

Fig. S4 Degradation curves of catalysts synthesized at a) different temperatures and b) atmospheres (Experimental conditions: $[H_2O_2]_0 = 2.0$ mM), [Catalysts] = 0.1 gL^{-1}, [Phenol] = 5 ppm, T = 25 °C and $pH_0 = 7$).

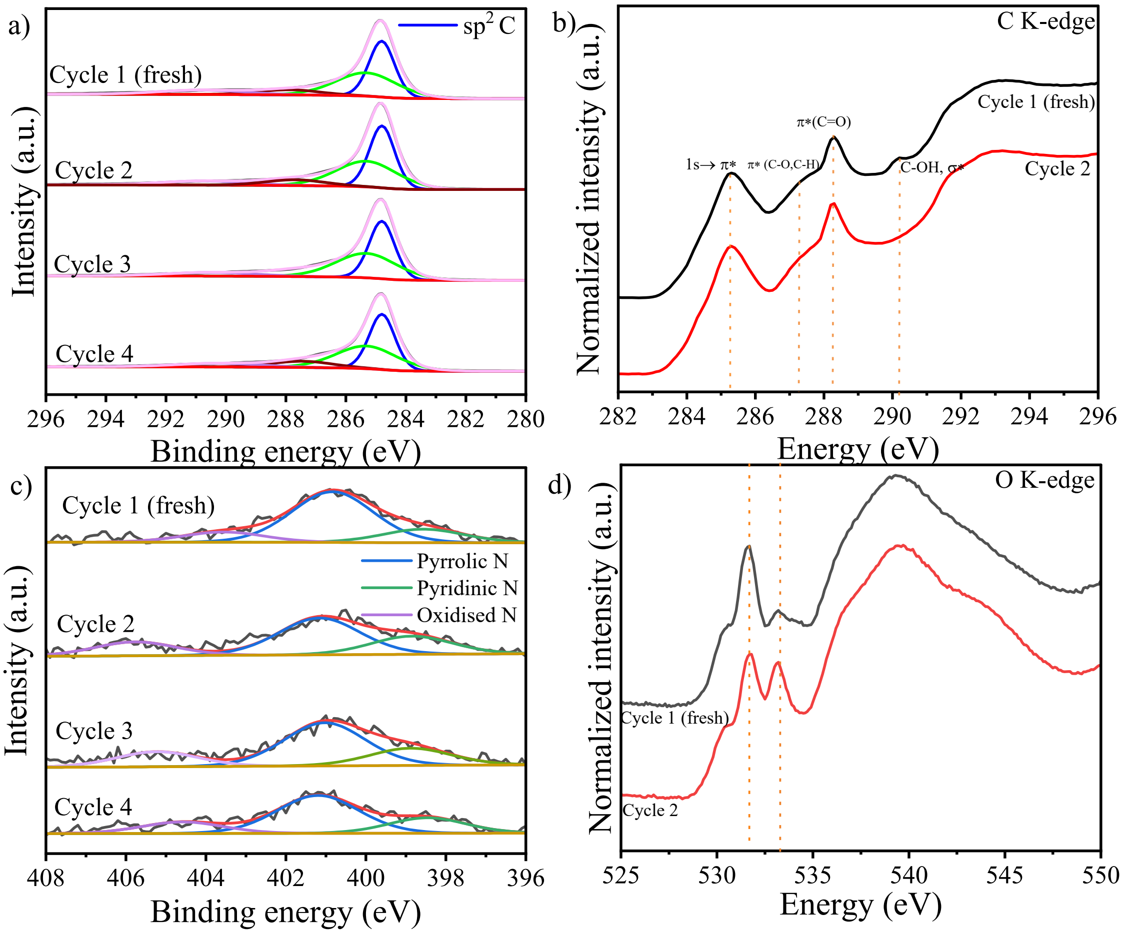

Fig. S5 a) High-resolution C 1s XPS, b) C 1s XANES spectra, c) high-resolution N 1s spectra and d) O1s XANES spectra of fresh and spent NH_3-C-900.

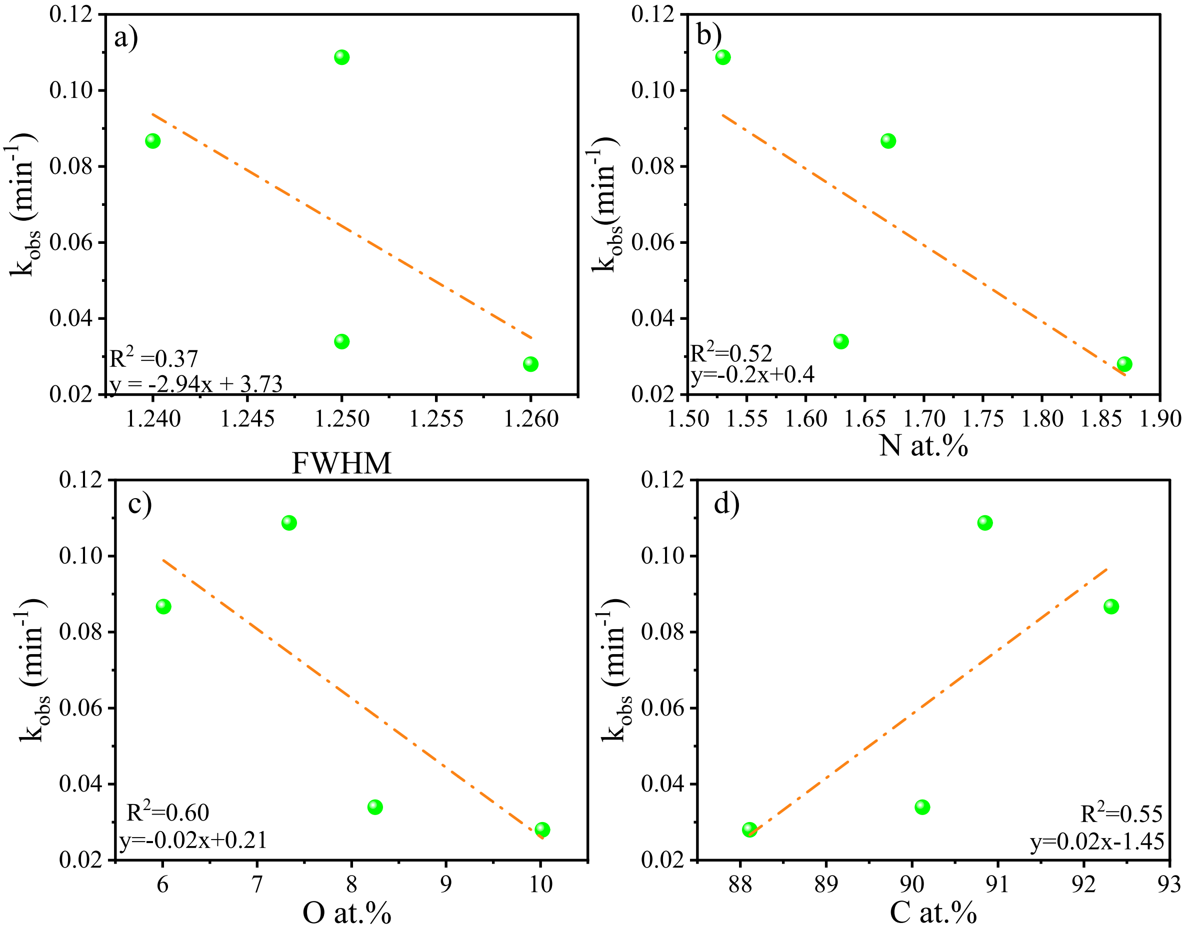

Fig. S6 Correlation of k_{obs} with (a) FWHM, (b) N at.%, (c) O at.% and (d) C at.%.

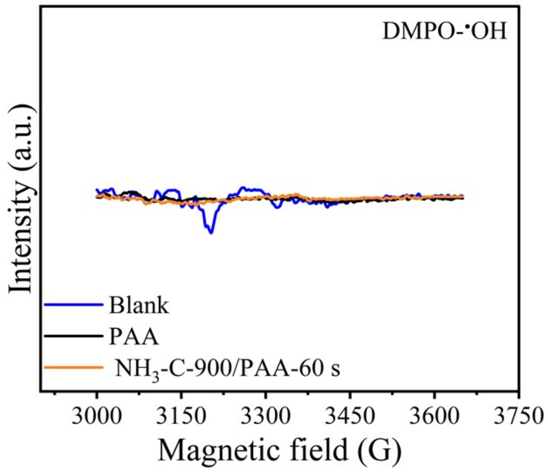

Fig. S7 EPR analysis in NH_3-C-900 /PAA system using DMPO as trapping agent. Conditions: [PAA] = 2 mM, [NH_3-C-900] = 0.1 g L^{-1}, [DMPO]= 50 mM, [Phenol] = 5 ppm, and T = 25 °C, pH_0 =7.

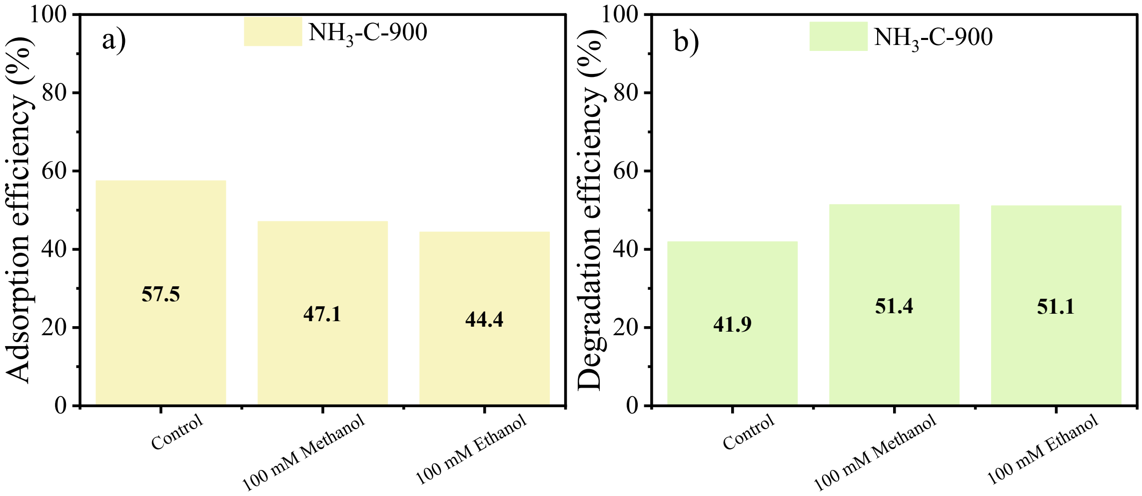

Fig. S8 a) Adsorption and b) degradation efficiency of phenol in 5 min in NH_3-C-900 /PAA system using MeOH and EtOH quenchers. (Experimental conditions: [PAA] = 2 mM, [Catalyst] = 0.1 gL^{-1}, [phenol] = 5 ppm, T = 25 °C and pH_0 =7)

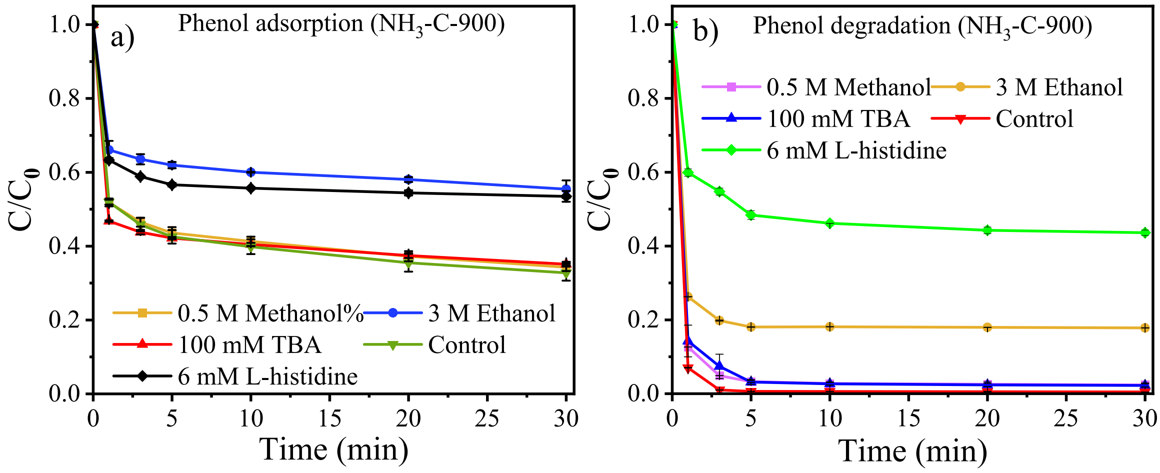

Fig. S9 Influence of quenching reagents on the a) adsorption and (b) degradation of phenol using NH_3-C-900 (Experimental conditions: [PAA] = 2 mM, [Catalysts] = 0.1 gL^{-1}, [phenol] = 5 ppm, T = 25 °C and pH_0 =7)

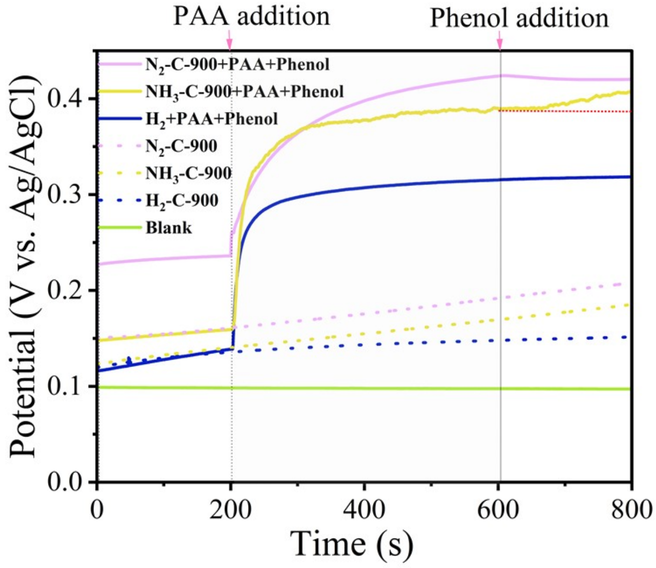

Fig. S10 OCP curves of different samples.

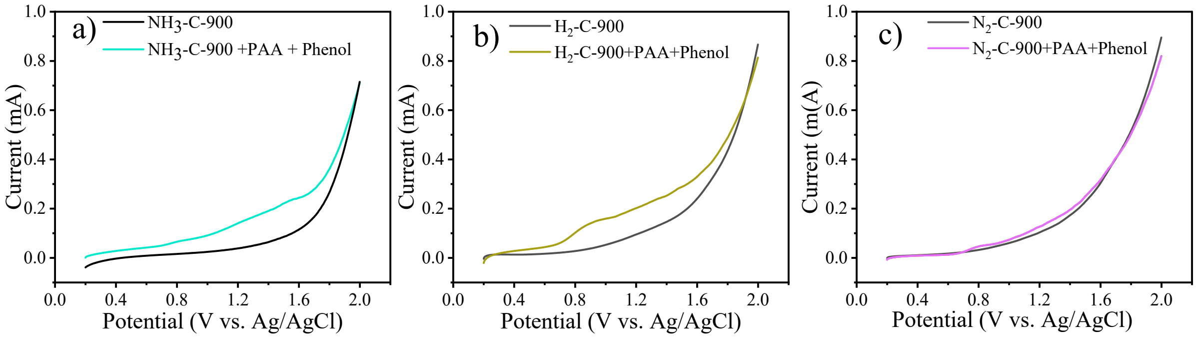

Fig. S11 Linear sweep voltammetry (LSV) curves of (a) NH_3-C-900, (b) H_2-C-900 and (c) N_2-C-900.

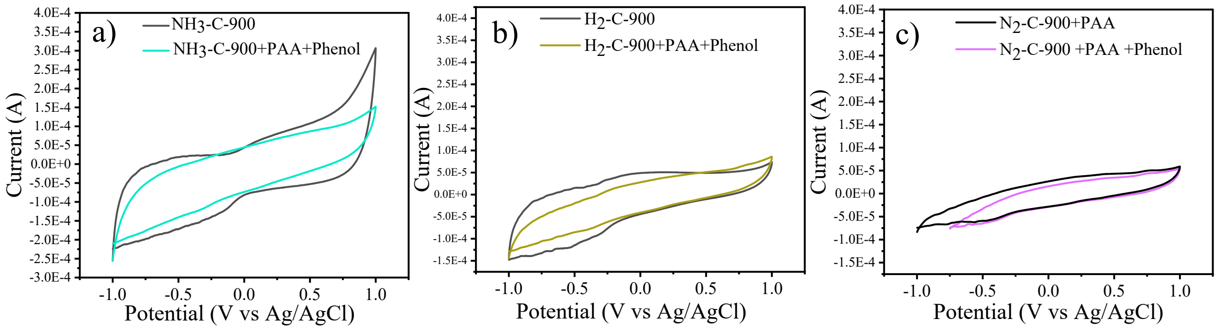

Fig. S12 The cyclic voltammetry (CV) curves of (a) NH_3-C-900, (b) H_2-C-900 and (c) N_2-C-900.

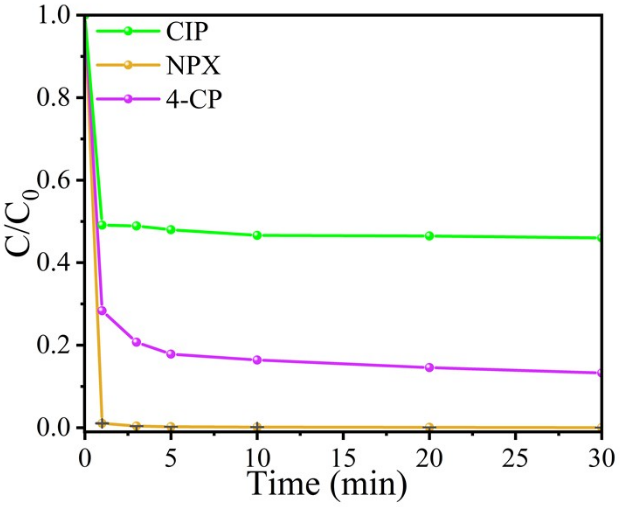

Fig. S13 Degradation of different micropollutants using the NH_3-C-900/ PAA system. Experimental conditions: [Catalyst] = 0.1 gL^{-1}, [PAA] = 2 mM, [Micropollutant] = 20 ppm, pH_0 =7.

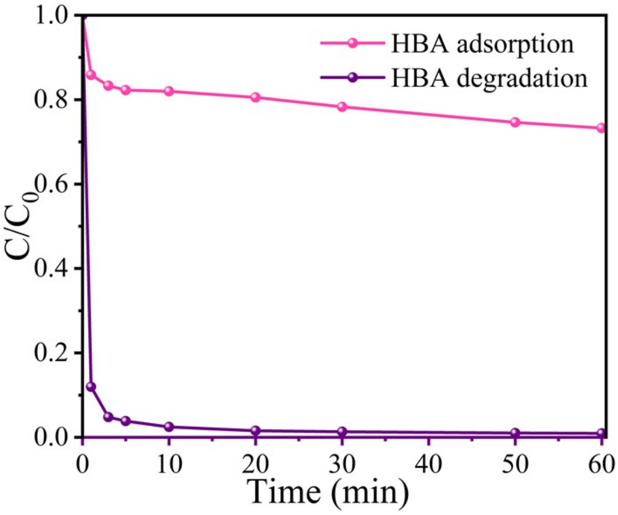

Fig. S14 Adsorption and degradation of HBA using the NH_3-C-900/ PAA system. Experimental conditions: [Catalyst] = 0.2 gL^{-1}, [PAA] = 2 mM (where required), [HBA] = 20 ppm, pH_0 =7.

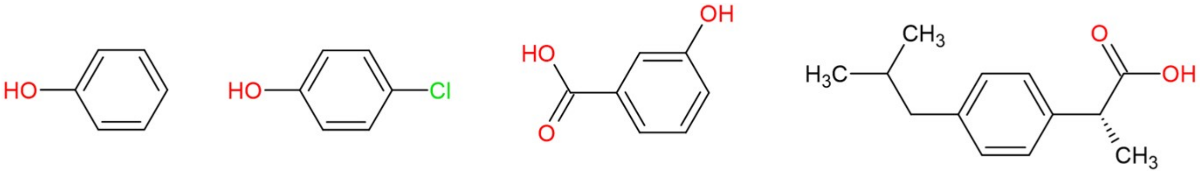

Phenol 4-chlorophenol Hydroxybenzoic acid Naproxen

Fig. S15 Chemical structure of phenol, 4-chlorophenol, hydroxybenzoic acid and naproxen.

Table S1 Physicochemical properties of the samples.

Samples	SSA/m^2 g^{-1}	V_t/cm^3 g^{-1}	V_{mic}/cm^3 g^{-1}	V_{meso}/cm^3 g^{-1}	C/at.%	N/at.%	O/at.%
N_2-C-500	111.41	0.07	0.04	0.03	86.13	1.53	12.34
N_2-C-600	209.20	0.11	0.08	0.03	88.25	1.18	10.57
N_2-C-700	318.04	0.15	0.12	0.03	88.34	1.35	10.31
N_2-C-800	451.42	0.22	0.17	0.05	89.41	0.97	9.62
N_2-C-900	444.04	0.24	0.16	0.08	89.60	1.16	9.24
N_2-C-1000	280.35	0.15	0.11	0.04	90.28	1.21	8.51
NH_3-C-900	816.14	0.39	0.31	0.08	90.85	1.53	7.62
H_2-C-900	511.04	0.24	0.19	0.05	92.29	0.98	6.73
Commercial AC	702.27	0.49	0.21	0.28	91.38	0.97	7.65

SSA was calculated using the BET method; total pore volume (V_t) was calculated at $P/P_0 = 0.99$; micropore volume (V_{mic}) was evaluated by the t-plot method; mesopore volume (V_{meso}) was obtained through the difference between V_t and V_{mic}.

Table S2 Chemical composition of fresh and spent NH_3-C-900 obtained from XPS results.

Sample	**(at. %)**				
	O 1s	**C=O**	**C–O**	**COOH**	
Cycle 1 (fresh)	7.34	4.35	2.77	0.22	
Cycle 2	6.01	2.13	3.45	0.47	
Cycle 3	8.25	1.168	6.62	0.46	
Cycle 4	10.02	1.80	7.66	0.56	
	N 1s	**Pyridinic N**	**Pyrrolic N**	**Oxidized**	
Cycle 1 (fresh)	1.53	0.35	0.90	0.27	
Cycle 2	1.67	0.30	1.14	0.23	
Cycle 3	1.63	0.43	0.87	0.33	
Cycle 4	1.87	0.37	1.07	0.43	
	C 1s	**C–C**	**C–OH**	**C=O**	**π–π* satellite**
Cycle 1 (fresh)	90.85	36.45	38.24	9.17	6.99
Cycle 2	92.32	37.16	39.34	9.80	6.02
Cycle 3	90.12	35.95	39.07	9.73	5.37
Cycle 4	88.11	35.09	37.76	10.05	5.21

References

1. D. Kong, Y. Zhao, H. Guo, M. Han, X. Fan, J. Li, X. He and J. Ma, *ACS ES&T Eng.*, 2023, **3**, 1030-1041.